JOURNAL OF GUIDANCE, CONTROL, AND DYNAMICS
Vol. 18, No. 4, July–August 1995

Experimental Application of an Explicit Optimal Linear Quadratic Gaussian Controller

John H. Lilly*
University of Louisville, Louisville, Kentucky 40292

This paper summarizes the results of some experiments performed on the Spacecraft Control Laboratory Experiment facility at NASA Langley Research Center using the explicit optimal linear quadratic Gaussian (LQG) control methodology. Explicit LQG is a method for controlling multi-input, multi-output flexible structures with collocated actuators and rate sensors. The model used for these experiments is a simple lumped model describing the motion of the reflector. The controller is tested on the first five (lowest frequency) modes of the structure. Significant improvement in damping results, the largest being a factor-of-300 improvement in mode 3 damping. Also, some characteristics of the theoretical closed-loop system are presented that enable greater insight into the properties of the explicit optimal LQG controller.

I. Introduction

THE Spacecraft Control Laboratory Experiment (SCOLE, dismantled in 1993)[1] is a large flexible antenna and associated control equipment located at NASA Langley Research Center in Hampton, Virginia. The antenna consists of a 10 ft., thin, flexible mast hanging vertically from either a movable or fixed connection point, together with a rigid "reflector" attached at right angles to the mast at the bottom (Fig. 1). The mast is connected to the reflector at one of the reflector's edges. SCOLE is equipped with collocated actuators (torque wheels) and sensors (rate gyroscopes) in each of the three axes of motion, which are the actuators and sensors used for these experiments, as well as a set of cold-gas jets and accelerometers, which were not used for these experiments.

SCOLE has been used by many researchers investigating various identification and control techniques for multi-input, multi-output (MIMO) flexible structures. In the experiments reported in this paper we seek to damp out vibrations in the antenna with the torque wheels by utilizing the explicit optimal linear quadratic Gaussian (LQG) control methodology of Balakrishnan,[2–4] which is applicable specifically to flexible structures with collocated actuators and rate sensors. The explicit optimal LQG method produces a compensator that can be expressed in lumped state-space form and is thus suitable for implementation on a digital computer. The compensator can also be shown to be positive real, making it robust to unmodeled dynamics.

We utilize for these experiments a simple lumped model for SCOLE that describes the motion of the reflector. We test the controller by first exciting the antenna in one of its modes, then turning off the excitation, closing the control loop, and recording the resulting motion. This is done for the five lowest frequency modes. For modeling purposes, we define a different coordinate system from that which has been traditionally used for SCOLE.

The simple lumped model used for these experiments was intended for initial tests only, with a more complete model planned once confidence was gained with the lumped one. Unfortunately, the untimely demise of Larry Taylor and the subsequent dismantling of SCOLE prevented any further experimentation. We nevertheless feel that the preliminary results obtained and reported in this paper are sufficient to show that explicit optimal LQG is a promising methodology for the regulation of MIMO flexible structures.

The paper is organized as follows. Section II gives a brief summary of the explicit LQG methodology. Section III gives a physical description of the SCOLE apparatus. Section IV discusses the modeling procedure. Section V describes the design of the compensator and gives some of the properties of the resulting theoretical closed-loop system. Section VI gives experimental results. Conclusions are given in Sec. VII.

II. Brief Summary of Explicit Optimal LQG Controller

The material presented here is taken from Refs. 2–5. We begin with the general model of an undamped flexible structure with collocated actuators and rate sensors:

$$M\ddot{x}(t) + Ax(t) + Bf(t) + BN_a(t) = 0 \tag{1a}$$

$$v(t) = B^T\dot{x}(t) + N_r(t) \tag{1b}$$

This model can describe either finite- or infinite-dimensional systems, depending on how the operators are defined. For finite-dimensional systems, M is the mass matrix (nonsingular, nonnegative definite), A is the stiffness matrix (nonsingular, nonnegative definite), B is the control matrix, $f(\cdot)$ is the control vector ($n \times 1$, assuming n actuators), $x(\cdot)$ is the "displacement" vector (finite-dimensional, real), $N_a(\cdot)$ is the actuator noise (assumed white Gaussian with spectral density $d_a I$), I is the $n \times n$ identity matrix, $v(\cdot)$ is the sensor output, B^T represents the transpose of B, and $N_r(\cdot)$ is the sensor noise (assumed white Gaussian with spectral density $d_r I$). For continuum models, see Ref. 5.

The LQG problem considered is that of finding the control $f(\cdot)$ that minimizes the mean-square time average (where $\lambda > 0$)

$$\lim_{T\to\infty}\left\{\frac{1}{T}\int_0^T \|B^T\dot{x}(t)\|^2\,dt + \frac{\lambda}{T}\int_0^T \|f(t)\|^2\,dt\right\} \tag{2}$$

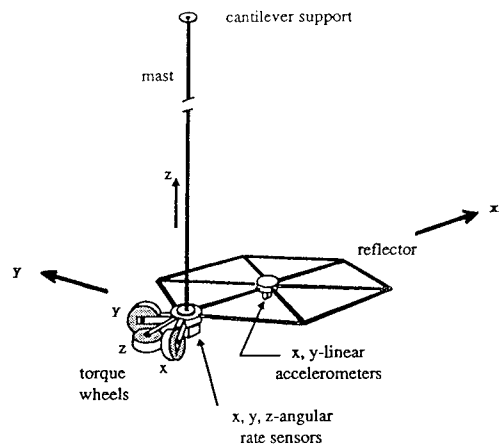

Fig. 1 Cantilevered SCOLE antenna showing torque wheels, rate sensors, and coordinate system used.

Received Nov. 15, 1993; revision received Aug. 1, 1994; accepted for publication Dec. 7, 1994.

*Associate Professor, Department of Electrical Engineering.

The optimal compensator is derived using stochastic optimization theory. The optimal compensator transfer function matrix ($n \times n$) is given by (see Ref. 2)

$$H(s) = sgB^T(s^2M + s\gamma BB^T + A)^{-1}B, \qquad \mathrm{Re}(s) > 0 \quad (3)$$

where

$$g = \sqrt{\frac{d_a/d_r}{\lambda}}, \qquad \gamma = \sqrt{\frac{d_a}{d_r}} + \frac{1}{\sqrt{\lambda}} \quad (4)$$

In the finite-dimensional case, the compensator (3) can be realized in the (finite-dimensional) state-space form

$$f(t) = gB^T\dot{Y}(t) \quad (5a)$$

$$M\ddot{Y}(t) + AY(t) + \gamma BB^T\dot{Y}(t) = Bv(t) \quad (5b)$$

This is the form of the compensator used in our experiments. It can be shown that the compensator given by Eq. (3) or (5) is positive real,[2] making it robust with respect to unmodeled dynamics.

III. SCOLE Physical Description

These experiments were performed with the SCOLE antenna in its cantilevered configuration, i.e., with the top end of the antenna fixed. Figure 1 (adapted from Ref. 6) shows the coordinate system used for modeling and controller derivation. The origin of the coordinate system is the attach point, i.e., the point of attachment between the mast and the reflector.

The states of the model are u_x (displacement of reflector in x direction), u_y (displacement of reflector in y direction), θ_x (angular velocity of reflector about x axis), θ_y (angular velocity of reflector about y axis), θ_z (angular velocity of reflector about z axis), and their derivatives. The displacement of the reflector in the z direction (u_z) is assumed negligibly small. The system input is introduced through three mutually orthogonal torque wheels situated at the attach point. The system output is sensed through three mutually orthogonal rate gyroscopes, collocated with the torque wheels. Thus, the system has input vector $f \sim 3 \times 1$ and output vector $v \sim 3 \times 1$. Note that the orientations of the x, y, and z torque wheels and rate sensors are different from our definitions of the x, y, and z axes. Thus, angular transformations were necessary in order to implement our compensator with these actuators and sensors.

The plane of the antenna is defined to be that formed by the x and z axes. In-plane motion refers to motion of the reflector in this plane (i. e., in the direction of the x axis), and out-of-plane motion refers to motion of the reflector normal to this plane (i.e., in the direction of the y axis). Torsion refers to twisting motion of the mast and reflector about the z axis.

It was found experimentally that the sixth mode and all higher frequency modes of SCOLE damp out within 2 s or less. Thus, we attempted to control only the first five modes in these preliminary experiments. These are listed in Table 1, with their experimentally measured frequencies and damping ratios.

IV. Modeling of SCOLE

The system is modeled in a manner similar to Ref. 7 from basic principles of physics, utilizing the physical properties and geometry of the SCOLE antenna. The model is assumed to be in the form of Eq. (1), where $x = [u_x\ u_y\ \theta_x\ \theta_y\ \theta_z]^T$:

Table 1 Experimentally measured open-loop frequencies and damping ratios for first five modes of SCOLE

Mode	Measured frequency, Hz	Measured damping ratio
1) First in-plane bending	0.4545	0.0018
2) First out-of-plane bending	0.4764	0.0061
3) First torsion	1.53	0.0005
4) Second in-plane bending	3.13	0.0106
5) Second out-of-plane bending	4.63	0.0077

$$M = \begin{bmatrix} m & 0 & 0 & 0 & 0 \\ 0 & m & 0 & 0 & mr_x \\ 0 & 0 & I_{xx} & 0 & 0 \\ 0 & 0 & 0 & I_{yy} + mr_x^2 & 0 \\ 0 & mr_x & 0 & 0 & I_{zz} + mr_x^2 \end{bmatrix} \quad (6)$$

$$A = \begin{bmatrix} \frac{12EI}{L^3} + \frac{1.2mg}{L} & 0 & 0 & \frac{6EI}{L^2} + \frac{mg}{10} & 0 \\ 0 & \frac{12EI}{L^3} + \frac{1.2mg}{L} & \frac{-6EI}{L^2} - \frac{mg}{10} & 0 & 0 \\ 0 & \frac{-6EI}{L^2} - \frac{mg}{10} & \frac{4EI}{L} + \frac{2mgL}{15} & 0 & 0 \\ \frac{6EI}{L^2} + \frac{mg}{10} & 0 & 0 & \frac{4EI}{L} + \frac{2mgL}{15} & 0 \\ 0 & 0 & 0 & 0 & \frac{EI_\psi}{L} \end{bmatrix} \quad (7)$$

$$B = \begin{bmatrix} 0 & 0 & 0 \\ 0 & 0 & 0 \\ 1 & 0 & 0 \\ 0 & 1 & 0 \\ 0 & 0 & 1 \end{bmatrix} \quad (8)$$

and m is the mass per unit length of the mast (0.8637 slug/ft), I_{xx} is the moment of inertia of the reflector about the x axis (0.5793 slug-ft^2), I_{yy} is the moment of inertia of the reflector about the y axis (1.1557 slug-ft^2), I_{zz} is the moment of intertia of the reflector about the z axis (1.7351 slug-ft^2), r_x is the distance from the reflector center of gravity to the attach point (0.39 ft), L is the length of the mast (10 ft), E is the modulus of elasticity of the mast, I is the cross-sectional moment of inertia of the mast, I_ψ is the cross-sectional polar moment of inertia of the mast, EI is the bending stiffness of the mast (1110 lb-ft^2), EI_ψ is the torsional stiffness of the mast (1.6096×10^3 lb-ft^2), and g is the acceleration of gravity (32.2 ft/s^2).

When the model is expressed in first-order ODE form, the poles of the model are $s = \pm j2.7322, \pm j2.7466, \pm j9.6576, \pm j19.636, \pm j29.037$. It will be noted that the model poles correspond to open-loop frequencies that are slightly different from the experimentally measured quantities in Table 1. Also, our model contains no damping, whereas the actual structure obviously does. Thus, our preliminary model is a simplistic one.

V. Compensator Design and Theoretical Closed-Loop Performance

The optimal compensator (5) can be rewritten in first-order ordinary differential equation (ODE) form as

$$\begin{bmatrix} \dot{Y} \\ \ddot{Y} \end{bmatrix} = \begin{bmatrix} 0 & I \\ -M^{-1}A & -\gamma M^{-1}BB^T \end{bmatrix} \begin{bmatrix} Y \\ \dot{Y} \end{bmatrix} + \begin{bmatrix} 0 \\ M^{-1}B \end{bmatrix} v(t) \quad (9a)$$

$$f(t) = gB^T\dot{Y} \quad (9b)$$

Table 2 Theoretical closed-loop poles, damped natural frequencies, and damping ratios resulting from compensator with $g = 12$, $\gamma = 10$

Mode	Theoretical closed-loop poles	Theoretical closed-loop frequency, Hz	Theoretical closed-loop damping ratio
1	$-.016936 \pm j2.7323$	0.4349	0.0061983
2	$-.016864 \pm j2.7467$	0.4372	0.0061396
3	$-.40292 \pm j9.6492$	1.5357	0.041720
4	$-.52476 \pm j19.629$	3.1241	0.026724
5	$-1.1856 \pm j29.011$	4.6172	0.040833

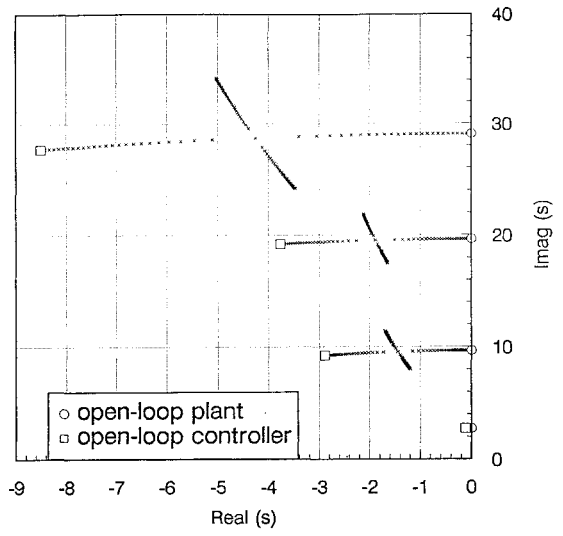

Fig. 2 Locus of closed-loop poles as g varies from 0 to 60 ($\gamma = 10$).

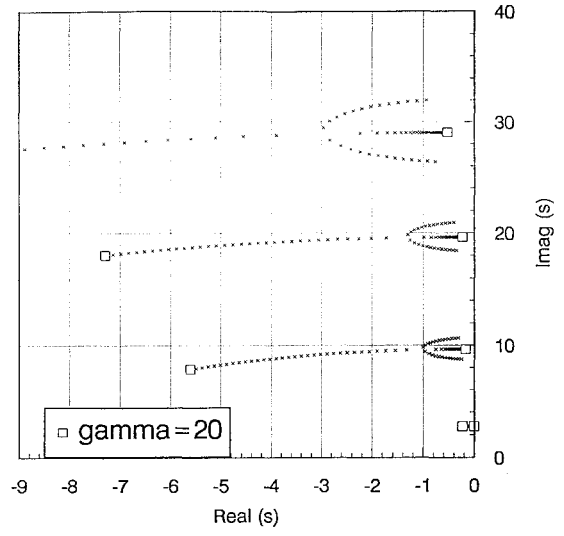

Fig. 3 Locus of closed-loop poles as γ varies from 20 to 2 ($g = 12$).

A sampling time of 0.02 s was chosen for the compensator. The compensator has 10 states, 3 inputs, and 3 outputs. The variables γ and g [Eq. (4)] are the only design parameters of the controller. The constant g is the gain of the compensator, whereas the compensator damping is proportional to γ. We considered a range of values for these constants. Nominal values of $g = 12$ and $\gamma = 10$ were chosen heuristically, since they were judged to yield the best closed-loop performance in actual experiments on SCOLE. These values of g and γ result in the theoretical (i.e., based on the model described above) closed-loop poles, damped natural frequencies, and damping ratios given in Table 2.

It is of interest to examine the loci of theoretical closed-loop poles as g and γ vary. Figure 2 shows the locus of theoretical closed-loop poles as g varies from 0 to 60 with γ held at its nominal value of 10. There are two closed-loop plant poles and two compensator poles very near the positive imaginary axis between approximately $s = j2.6$ and $s = j2.9$. The loci corresponding to these poles are similar to the others in Fig. 2. Figure 3 shows the locus of closed-loop poles as γ varies from 20 to 2 with g held at its nominal value of 12.

The transmission zeros of the compensator are $s = 0, 0, 0 \pm j4.3917, \pm j4.3917$ and are γ-invariant. Note that these do not coincide with any open-loop plant poles. This is desirable, because any cancellation of plant poles by compensator zeros would result in uncontrollable plant modes.

One objective of the compensator is to minimize the sensitivity of the system to actuator and sensor disturbances (N_a and N_r, respectively). This sensitivity can be investigated by examining a plot of the largest principal gain $\bar{\sigma}(\omega)$ of the transfer matrix of the appropriate disturbance-to-output path. The principal gains of a transfer matrix $G(s)$ are defined to be the singular values of $G(j\omega)$ as a function of ω.[8] The smaller is $\bar{\sigma}(\omega)$, the less is the sensitivity. Figure 4 shows $\bar{\sigma}(\omega)$ for the actuator-to-output (i.e., N_a-to-v) transfer matrix of the theoretical closed-loop system. Note that the first two modes are very close together in frequency and therefore appear as one peak in Fig. 4. The first four modes are seen to be relatively insensitive to actuator noise, whereas the fifth mode is somewhat more sensitive. It is not known why the fifth mode is more sensitive. Of course, the theoretical (i.e., zero damping) open-loop system, to which this theoretical closed-loop system should be compared, would have infinitely high peaks at the mode frequencies. The N_r-to-v maximum principal-gain plot is similar to Fig. 4 and is therefore omitted.

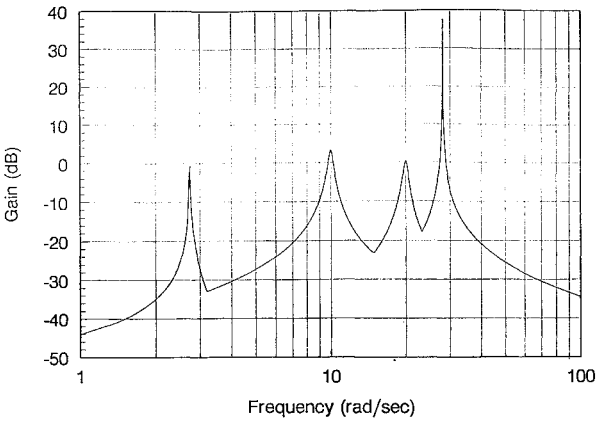

Fig. 4 Maximum principal gain of actuator-to-output transfer matrix of compensated plant ($g = 12$, $\gamma = 10$).

VI. Experimental Results

The experiments were run as follows. First, the antenna was excited for 30 s in the desired mode by commanding the torque wheels with a sinusoid at the appropriate frequency. Then the excitation was turned off, the controller loop was closed, and the rate gyroscope outputs recorded. The constants g and γ were varied over a large range of values. The best closed-loop performance was obtained for $g = 12$ and $\gamma = 10$. The approximate closed-loop damped natural frequencies and damping ratios in Table 3 were derived from the measurements using these values for g and γ.

Table 3 Experimentally measured closed-loop damped natural frequencies and damping ratios, $g = 12$, $\gamma = 10$

Mode	Measured closed-loop frequency, Hz	Measured closed-loop damping ratio
1	0.4528	0.0531
2	0.4589	0.0309
3	1.5568	0.1567
4	3.2215	0.1607
5	4.5405	0.2326

These numbers should be compared to those for the open-loop system in Table 1. A comparison of the open-loop and the closed-loop damping ratios gives an idea of the effectiveness of the compensator. The compensator significantly enhanced the damping in all modes. The largest improvement was obtained in mode 3, which is the least stable in open-loop performance. Mode 3 damping was improved by a factor of approximately 300. The smallest improvement was obtained in mode 2, whose damping was increased by a factor of 5.

It will be noticed that the agreement between the damping ratios in Tables 2 and 3 is not very good. This is because the model includes no damping while the actual system does contain some damping. Thus, the actual performance obtained is better than that expected theoretically.

VII. Conclusions

The explicit optimal LQG control methodology has been implemented on the SCOLE flexible antenna. A simplistic lumped model was used to derive the compensator. The compensator was tested on the first five modes of the antenna. It resulted in significant improvement in damping in all modes. The largest improvement in damping was a factor-of-300 improvement in mode 3. The smallest improvement was a factor-of-5 improvement in mode 2. It is significant that the controller yielded excellent improvement even in the face of inaccuracies introduced by using such a simplistic model.

Acknowledgments

This research was supported by NASA, Research Grant NAG-1-1446. The author also acknowledges the help of Larry Taylor (deceased) of NASA Langley Research Center, Hampton, Virginia. Mr. Taylor gave freely of his time and guidance in helping to accomplish this research. He has immeasurably helped me and many of my colleagues in our research and our careers, and we are grateful.

References

[1]Taylor, L. W., and Balakrishnan, A. V., "A Mathematical Problem and a Spacecraft Control Laboratory Experiment (SCOLE) Used to Evaluate Control Laws for Flexible Spacecraft—NASA/IEEE Design Challenge," *Proceedings of the NASA SCOLE Workshop,* Hampton, VA, 1984.

[2]Balakrishnan, A. V., "Compensator Design for Stability Enhancement with Collocated Controllers," *IEEE Transactions on Automatic Control,* Vol. 36, No. 9, 1991, pp. 994–1007.

[3]Balakrishnan, A. V., "An Explicit Solution to the Optimal LQG Problem for Flexible Structures with Collocated Rate Sensors," presented at the Fifth NASA/DOD CSI Technology Conference, Lake Tahoe, CA, 1992.

[4]Balakrishnan, A. V., "Explicit LQG Optimized Control Laws for Flexible Structures/Collocated Rate Sensors," *Proceedings of the AIAA/ASME/ASCE/AHS/ASC 34th Structures, Structural Dynamics and Materials Conference* (La Jolla, CA), AIAA, Washington, DC, 1993.

[5]Balakrishnan, A. V., *Applied Functional Analysis* 2nd ed., Springer–Verlag, Berlin, 1981.

[6]Shenhar, J., and Montgomery, R. C., "Analytic Redundancy Management for Large Flexible Structures," *Proceedings of the VPI & SU Symposium on Dynamics and Control of Large Structures*, Blacksburg, VA, 1991.

[7]Taylor, L. W. and Leary, T., "On Incorporating Damping and Gravity Effects in Models," *Proceedings of the Third Annual NASA SCOLE Workshop* (Hampton, VA), 1986, pp. 121–148.

[8]Maciejowski, J. M., *Multivariable Feedback Design,* Addison–Wesley, Reading, MA, 1989.